Atmos. Chem. Phys. Discuss., 15, 19197–19238, 2015
www.atmos-chem-phys-discuss.net/15/19197/2015/
doi:10.5194/acpd-15-19197-2015

Atmospheric Chemistry and Physics
Discussions
Open Access

Changes in chemical components of aerosol particles in different haze regions in China from 2006 to 2013 and contribution of meteorological factors

X. Y. Zhang, J. Z. Wang, Y. Q. Wang, H. L. Liu, J. Y. Sun, and Y. M. Zhang

Key Laboratory of Atmospheric Chemistry, Institute of Atmospheric Compositions, Chinese
Academy of Meteorological Sciences, CMA, 46 Zhong Guan Cun S. Ave.,
Beijing 100081, China

Received: 29 May 2015 – Accepted: 17 June 2015 – Published: 13 July 2015

Correspondence to: X. Y. Zhang (xiaoye@cams.cma.gov.cn)

Published by Copernicus Publications on behalf of the European Geosciences Union.

Abstract

Since individuals experienced persistent haze-fog events in January 2013 in central-eastern China, questions on factors causing differences in drastic changes in 2013 from those in adjacent years have been raised. Changes in major chemical components of aerosol particles over the years also remain unclear. The extent of meteorological factors contributed to such changes is yet to be determined. The study intends to present the changes in daily-based major water-soluble constituents, carbonaceous species and mineral aerosol in PM_{10} at 13 stations within different haze regions in China from 2006 to 2013, associated with specific meteorological conditions that are highly related with aerosol pollution (parameterized as an index called "PLAM"). No obvious changes were found in annual mean concentrations of these various chemical components and PM_{10} in 2013, relative to 2012. By contrast, wintertime mass of these components were quite different, in Hua Bei Plain (HBP), sulfate, OC, nitrate, ammonium, EC, and mineral dust concentrations in winter were approximately 43, 55, 28, 23, 21 and 130 $\mu g\, m^{-3}$, respectively; these masses were approximately two to four times higher than those in background mass, also exhibiting a decline during 2006 to 2010, and then a rise till 2013. The mass of these concentrations and PM_{10}, except mineral, respectively increased by approximately 28 to 117 and 25 % in January 2013 compared with that in January 2012. Thus, persistent haze-fog events occurred in January 2013, and approximately 60 % of this increase in component concentrations from 2012 to 2013 can be attributed to severe meteorological conditions in the winter of 2013. In Yangtzi River Delta (YRD) area, winter masses of these components, unlike HBP, did not significantly increase since 2010; PLAM was also maintained at a similar level without significant changes. In the Pearl River Delta (PRD) area, the regional background concentrations of the major chemical components were similar to those in YRD; accounted approximately 60–80 % of these in HBP. Since 2010, a decline was found for winter concentrations, which can be partially attributable to a persistent bettering me-

teorological conditions and the emission cutting with an emphasis on coal-combustion in this area.

In addition to the scattered and centralized coal-combustion for heating, burning biomass fuel contributed to the large increase in the concentrations of carbonaceous aerosol in major haze regions, except in PRD, in winter. No obvious changes were found for the proportions of each chemical components of PM_{10} from 2006 to 2013. Among all of the emissions recorded in chemical compositions in 2013, coal-combustion was still the largest anthropogenic source of aerosol pollution in various areas in China, with higher sulphate proportion of PM_{10} in most areas of China. OC normally ranked the third. PM_{10} concentration increased by approximately 25 % in January of 2013 relative to 2012 that caused persistent haze-fog events in HBP; emission also reduced by approximately 35 % in Beijing and its vicinity (BIV) in late fall of 2014, thereby producing “APEC” blue; thus one can expect that the persistent haze-fog events would be reduced significantly in the BIV, if ~ one-third of the 2013 winter emission could be reduced, which can also be viewed as the upper limit of atmospheric aerosol pollution capacity in this area.

1 Introduction

From satellite-based aerosol optical depth, ambient fine particulate matter concentrations were found to have a high loading area with China as major body in the word (Donkelaar and Villeneuve, 2010). Globally, mass concentrations of six major types of chemical components in aerosol particles in China were also found to be just lower than those in urban S. Asian area but far higher than those in Europe and N. America (Zhang et al., 2012a), with large variation in time and space (He et al., 2001; Hu et al., 2002; Yao et al., 2002; Ye et al., 2003; Zhang et al., 1993, 2002, 2008; Li et al., 2014; Xu et al., 2014; Yin et al., 2012). Moreover, approximately 37.5 billion tons of standard coal are consumed as energy source in China; approximately 66 % of the produced energy was attributed to coal consumption in 2013 (NBS-China, 2014). Because the aerosol particles and cloud (fog) droplet can influences atmospheric visibility (Watson, 2002); and in the ambient atmosphere, no cloud (fog) can be formed if no hygroscopic aerosols can be activated to cloud condensation nuclei (CCN) or ice nuclei (IN) (Twomey, 1977; Seinfeld and Pandis, 1997), high loadings of aerosols not only affect climate change (Forster et al., 2007; Boucher et al., 2013), but also adversely influence weather (Wang et al., 2010; Pérez et al., 2006) and contribute to the occurrence of haze and fog events; both of them can be considered as types of aerosol pollution in present day China (Zhang et al., 2013). Since individuals experienced persistent haze-fog events in January 2013 in central-eastern China, the change of aerosol particles and their chemical component are attracting special attentions in this rapid economic growth and high population density area (Huang et al., 2014; Zhang et al., 2013; Guo et al., 2014; H. Wang et al., 2014; X. Wang et al., 2014; Z. Wang et al., 2014; Wang et al. 2015; Sun et al., 2014). However, questions was raised about what changes happened to the major chemical components of aerosol in different haze areas in China during recently year? Why a big difference existed in 2013 and an adjacent year in the case of no significant changes in emission? What extent of meteorological factors contributed to the change?

China can be classified into nine typical regions with similar visibility changes in each (Zhang et al., 2012a); four of these regions have experienced the largest loss of visibility in recent decades, particularly (1) Hua Bei Plain in North China and Guanzhong Plain. This region also includes “Jing–Jin–Ji” or called “Beijing–Tianjin–Hebei” (BTH) region with the rapid economic development; this area is also considered as Haze Region II in China, (2) East China with the main body in Yangtze River Delta area (Haze Region III), (3) South China comprising Guangdong and Pearl River Delta area (Haze Region V), (4) Si Chuan Basin in Southwest China (Haze Region VI) (Fig. 1). Changes in major chemical components of aerosol in these different haze areas also remain unknown. These changes are also important to explore the reasons of the occurrence of severe haze-fogs in China in recent years.

Various meteorological factors, including wind speed, wind direction, air pressure, temperature, humidity, precipitation, and atmosphere stability, are possibly related to aerosol pollution, but each meteorological factor cannot completely and quantitatively indicate the integrated situation of meteorological conditions that may aggravate aerosol pollution (Sui et al., 2007; Pang et al., 2009). However, mechanisms by which these meteorological impacts can be quantified and by which these data can be used to diagnose aerosol pollution based on a longer time scale of emission changes than meteorological factors (Wang et al., 2012; Yang, 2009).

Long-term daily-based aerosol chemical components were determined here for aerosol particles with diameter less than 10 µm (PM_{10}) from regionally representative measurement networks (China Atmosphere Watch network-CAWNET) from 2006 to 2013. The parameterized index (PLAM) (Wang et al., 2012; Yang, 2009) was also used in this study to evaluate specific meteorological conditions and their connections with severe aerosol pollution. This study investigates the changes and the extent of these changes by analyzing chemical component changes and meteorological factors; this study also determined the relative contribution of specific meteorological conditions in winter. These chemical component data, especially in 2012 and 2013, can also be used as a basis to evaluate various control measures that have been used. After 2013, the Chinese government promoted ten prevention and countermeasures for aerosol pollution control called “Atmospheric Pollution Prevention and Control of the Ten Measures of China.” The government also released the Second Atmospheric Pollution Control Special Plan. All these have gained increasing attention among researchers to reduce emission caused by aerosol with an emphasis on coal combustion and industrial manufacturing processes, mainly in steel mills, chemical plants, glass, and cement plants. The long-term chemical characterization of aerosols in China is also essential to assess the effect of aerosols in the atmosphere and climate, and the results can be used to evaluate and improve existing haze-fog forecasting systems.

2 Sample collection and analyses

2.1 Sampling description

24 h aerosol filter samples were collected at 13 CAWNET stations on a one day in every three day basis from 2006 to 2013. These CAWNET stations are operated by the China Meteorological Administration (CMA), as shown in Fig. 1 and the details of these stations have been reported in previous studies (Zhang et al., 2012a, 2008). Aerosol samples were collected by using MiniVol™ air sampler (Airmetrics, Oregon USA) operated at an ambient air flow rate of 5 L min^{-1} for 24 h from 9:00 a.m. to 9:00 a.m. (BST) the following day. The filtration media were 47 mm Whatman quartz microfibre filters (QM/A) that were cleaned by heating at 800 °C for 3 h before use.

2.2 Aerosol chemical component analyses

The elemental concentrations were analyzed directly via X-Ray Fluorescence (XRF) method using X-Lab 2000 (SPECTRO, Germany) at the Key Laboratory for Atmospheric Chemistry (LAC), Chinese Academy of Meteorological Sciences (CAMS). Eighteen elements, namely, As, Br, Ca, Cr, Cu, Fe, K, Mg, Mn, Na, Ni, Pb, S, Se, Ti, V, Zn and Zr were analyzed using a Multi-Channel Analyzer that was calibrated using a standard plastic sample to check the signal energy and the multi-channel twice a month. The XRF spectrometer includes a high-tech detector using a silicon lithium drifted crystal cooled at a low temperature (−90 °C). This crystal is able to discriminate between X-ray photons of different energies, i.e. energy dispersion. Four different targets (Mo, Co, Al_2O_3, and Highly Oriented Pyrolytic Graphite (HOPG)) with different energy are employed to identify different elements. For the Mo target, the energy range is 25 keV, which is suitable for Cr, Mn, Fe, Co, Ni, Cu, Zn, As, Se, Br, Pb and Zr. The Al_2O_3 target with a working energy of 50 keV is deal for Cd, Sb and Ba while the Co target has an energy range of 12.5 keV for the analysis of K, Ca, Ti, V, Cr, Mn. The HOPG target's working tube voltage is 12.5 keV, which is good for Na, Mg, Al, P, S and Cl. Eighteen elements, i.e. As, Br, Ca, Cr, Cu, Fe, K, Mg, Mn, Na, Ni, Pb, S, Se, Ti, V, Zn and Zr, were analyzed by the Multi-Channel Analyzer. A standard glass sample (Spectro Corp. Germany) was used to check the signal energy and the multi-channel twice a month. The standard calibration curve between the intensity of signal and the elemental concentration is determined by single-element Mylar filters. Seven blank quartz filters were analyzed with Mylar matrices method. The averaged background of blank filters was subtracted during spectral processing. The detailed procedures at (LAC, CAMS) can be found in previous studies (Zhang et al., 2012a).

After XRF analysis, a portion of the filter samples was extracted with 25 mL of double-deionized water (DDI) using a 3″ × 5″ clean-room Poly bag (Clean Room Products, In., Ronkonkoma, NY). The resulting extracts were analyzed for SO_4^{2-}, NO_3^-, NH_4^+ and other ionic species, including Na^+, K^+, Ca^{2+}, Mg^{2+}, F^- and Cl^- by ion chromatography (Dionex JCS 3000) with a OmniPac Pax-500 column, 25 mM H_2SO_4 autoregenerant, gradient elution (from 5 to 28.75 mM NaOH/5 % methanol) at the Key Laboratory of Atmospheric Chemistry, CMA. The detailed protocol can be found in a previous study (Zhang et al., 2002).

Thermal/optical reflectance carbon (TOR) analysis method for element carbon (EC) and organic carbon (OC) content was performed following the Interagency Monitoring of Protected Visual Environments (IMPROVE) protocol (Chow et al., 1993, 2004). The sample filter was heated stepwise at temperatures of 120 (OC1), 250 (OC2), 450 (OC3), and 550 °C (OC4) in a non-oxidizing (He) atmosphere, and at 550 (EC1), 700 (EC2), and 800 °C (EC3) in an oxidizing atmosphere of 2 % oxygen and 98 % He. Evolved carbon is oxidized to CO_2, and then reduced to CH_4 for detection by FID. The pyrolyzed or charred OC is monitored by reflectance at $\lambda = 633$ nm. The portion of EC1 until the laser signal returns to its initial value is assigned to pyrolyzed organic carbon (OP). The OC is defined by the sum of OC1, OC2, OC3, OC4, and OP while the EC is defined by EC1+EC2+EC3-OP. The detailed procedures at (LAC, CAMS) can be found in previous studies (Zhang et al., 2008).

Title Page
Abstract | Introduction
Conclusions | References
Tables | Figures
◀| |▶
◀ ▶
Back | Close
Full Screen / Esc
Printer-friendly Version
Interactive Discussion

2.3 Parameterized a index (PLAM) for evaluating specific meteorological condition that resulted in severe aerosol pollution

In this study, we used a parameterized index, namely, Parameter Linking Aerosol Pollution and Meteorological Elements (PLAM), which was derived from a relationship of PM_{10} and key meteorological parameters from 2000 to 2007 from various region of China by our group. The PLAM index has been used to evaluate the contribution of meteorological factors to changes in atmospheric composition and optical properties over Beijing during the 2008 Olympic Games (Zhang et al., 2009), and to identify the contribution of specific meteorological factors to the ten-day haze-fog event in 2013 (Zhang et al., 2013). Based on a set of weather sensitive parameters, an integrated index "PLAM" was parameterized (Wang et al., 2012; Yang, 2009). Among these factors, high temperature, high humidity, moderate wind, and high stability were the most relevant to the poor air-quality in China. The PLAM was thus established as a function of the following parameters:

$$\mathrm{PLAM}(F) \in f(p, t, w, \mathrm{rh}, e, s, c'\_, \ldots) \qquad (1)$$

where p, t, w, rh, e, s, and $c\_$ represent air pressure, air temperature, winds, relative humidity, evaporability, stability, and effective parameter associated with the contribution of air pollution $\beta(c')$, respectively.

A stable summer weather with high air temperature, high relative humidity, moderate winds, and stability might create a microenvironment for high PM_{10} concentrations in August over Beijing (Yang, 2009), and this climate corresponds to static dynamic forcing (baroclinicity) and thermal forcing (equivalent potential temperature (θe) gradient) in moist adiabatic processes in the atmosphere (Gao et al., 2004). Part of the temperature profile is between the adiabatic lapse rate (neutral stability) and the isothermal lapse rate (Johnson and Baker, 1997). Condensation is also a key factor that contributes to intense pollution at given weather conditions in the moist adiabatic processes in the atmosphere. Apparently, the final PLAM can be attributed to two major separate factors: (1) initial meteorological conditions $\alpha(m)$ associated with the atmospheric condensation processes and (2) a dynamic effective parameter associated with the initial contribution of air pollution $\beta(c\_)$ such as:

$$\mathrm{PLAM} = \alpha(m) \times \beta'(c). \tag{2}$$

The details have been described in the reference (Wang et al., 2012; Yang, 2009).

3 Results and discussion

3.1 Spatial distribution of chemical components

The CAWNET observational network covers all areas of China with 30 ground-based stations that have been operating since 2006. The concentrations of SO_4^{2-}, OC, NO_3^-, NH_4^+, EC, and mineral aerosol were measured in this paper by using PM_{10} filter samples collected from 13 stations, which are located in Haze Region I (Dalian), Haze Region II (Gucheng, Zhengzhou and XiAn), Haze Region III (LinAn, Jinsha and Change), Haze Region V (Panyu and Nanjing), Haze Region VI (Chengdu), Haze Region VIII (Lasha, but data in this study were just from 2006 to 2010), and Haze Region IX (Gaolanshan and Dunhung) (Fig. 1, and Zhang et al., 2012a). Mineral aerosol was the largest component in almost all stations based on the five-year average data from 2006 to 2010 (Fig. 2a). Thus, high "dust" is a character in aerosol pollution in China. In general, a high mineral concentration was observed in northwest China, thereby indicating the influence of dust from natural Asian dust sources. However, in the southern margin of the Loess Plateau in XiAn, the mineral level exceeded those in stations closer to natural dust sources (Dunhuang, Galanshan etc). Thus, urban fly coal ash and fugitive dust sources were also observed to affect the mineral levels in these areas. Based on the measurement results of non-crustal Ca in coarse particle fractions, especially during non-spring seasons (with fewer occurrences of Asian sand and dust storm (SDS)), part of the mineral dust is hypothesized to originate from construction activities and coal ash (Zhang et al., 2002). As such, even in the southern part of China, where the influence of Asian dust is low, the concentrations of these minerals are still significant. Mineral dust was characterized by using the surrogate concentration of Fe, which is around 4 % in the Chinese mineral dust mass (Zhang et al., 1993, 2003), although the uncertainties are still present.

The highest mean concentrations of SO_4^{2-} in aerosol particles from 2006 to 2010 were larger than 33 $\mu g\,m^{-3}$ at the urban stations of XiAn, Zhengzhou in Haze Region II, and at Chengdu of Haze Region VI. This result indicates that the effect of coal combustion emission was high in these areas (Fig. 2a). The lowest concentrations ($< 6\,\mu g\,m^{-3}$) were observed in the western desert area (Dunhuang) and the Tibetan Plateau (Lasha). Thus, the effect of coal combustion is low. The spatial patterns of total inorganic ammonia ions (NH_4^+) in China are fairly similar to those of SO_4^{2-} and NO_3^-. Aside from XiAn, Zhengzhou, and Chengdu, stations with high NO_3^- concentrations also include those further north of China (Gucheng and Dalian) with concentrations $> 11\,\mu g\,m^{-3}$, even at Panyu in Pearl River Delta area of the Haze Region V, mainly because of the influences from both motor vehicle and coal-combustion as well as natural gas burning (reason discussed later).

The concentrations of OC and EC are similar to the distribution of SO_4^{2-}, and the highest concentrations of OC (20 to 30 $\mu g\,m^{-3}$) and EC (7 to 10 $\mu g\,m^{-3}$) at XiAn, Zhengzhou, Gucheng, and Chengdu, in Haze Region II and Haze Region VI in south-western China, and the lowest concentrations were observed in rural northwest China and at the Tibetan Plateau. These higher levels are typically observed in regions with a high population density and are associated with emissions from biomass burning, traffic, and power generation (Zhang et al., 2012a).

3.2 Chemical proportions of PM_{10} and their changes from 2006 to 2013

From Fig. 2b, the highest concentrations of PM_{10} during 2013 were observed at urban stations of XiAn (~ 320 $\mu g\,m^{-3}$), followed by 200 to 240 $\mu g\,m^{-3}$ at Gucheng and

Zhengzhou. These stations are all located in Haze Region II (the HBP area), which is considered as the most seriously polluted region in China in terms of aerosol pollution. This result is similar with those obtained from 2006 to 2007 (Zhang et al., 2012a). In rural northwest China (Gaolanshan and Dunhuang station), the PM levels (240 to 250 $\mu g\,m^{-3}$) remain high, but chemical compositions are different with higher mineral fractions. In the Yangtze River Delta area in central eastern China (LinAn, Jinsha and Changde) of the Haze Region III, the PM levels (70 to 90 $\mu g\,m^{-3}$) were 3 times lower than those in the HBP, but the stations in Haze Region III are located in rural areas and those in the HBP are in urban areas. In the Chengdu urban station located in Haze Region VI, which is also called Si Chuan Basin (SCB) area in southwestern China, the PM level went up ~ 160 $\mu g\,m^{-3}$, and this value is between the level of Gucheng (200 $\mu g\,m^{-3}$) and Dalian in N. E. China in Haze Region I (90 $\mu g\,m^{-3}$). Thus, SCB is considered to be another polluted region in China, followed by N. E. China. The urban PM level in Haze Region V (PRD aras), with values of ~ 90 $\mu g\,m^{-3}$ at Panyu and Nanning, were similar to those in rural areas in Haze Region III, thereby showing that the area has a relatively low aerosol pollution in 2013.

During 2013, mineral dust was still the dominant fraction over various regions with a relatively high proportion, especially in rural northwest China (Gaolanshan and Dunhuang). Mineral dust accounted for about 75 to 85 % of PM_{10}. In other areas, the percentage was between 25 and 50 %.

In most of areas of China except rural northwest China, sulphate contributed the second, and the first large anthropogenic, mass fraction to the atmospheric aerosol with a range of 12 to 25 %. In other three stations (Gucheng, XiAn and Panyu), the sulphate fraction were bit lower than OC and ranked the third with a range of about 9–16 % (Fig. 2b). As such, coal combustion was still the largest anthropogenic source of aerosol pollution in various areas of China during 2013. These sulfate proportions and related conclusions are quite similar to those from our previous study, where we mainly focused on the classification of sources of aerosol in various regions in China from 2006 to 2007 (Zhang, 2014; Zhang et al., 2013), and from 2007 to 2008 in urban

Beijing (Zhang et al., 2012b). Table 1 shows the proportion change of each chemical component of PM_{10} at Haze Region II (Gucheng). No evident changes were observed from 2006 to 2013, again indicating that the sources of aerosol particles did not significantly change from 2006 to 2013. This result was also observed in other major haze regions in China, but that in northwest China (Gaolanshan and Dunhuang) is slightly different.

In Fig. 2b, OC normally ranked the third and accounted for about 7–19 % in terms of mass, with high proportions in Gucheng (19 %) and Panyu (16 %) in 2013. This value is also similar to that from 2006 to 2007 (Zhang et al., 2013). In the rural northwest China, OC accounted ∼ 8 %. In the urban and rural areas of China, about 55 and 60 % of OC can be attributed to secondary organic carbon (SOC) formed from volatile organic gases (VOCs), which mainly originate from chemical plants, paint and coatings, motor vehicle (including leaks during fuel), and vegetation from natural sources (Zhang et al., 2012a). The other half of OC is primary organic carbons (POCs) originating from coal combustion. Based on the emission inventory of Beijing and its vicinity (BIV) (Cao et al., 2010), about 55 % of POC emission can be attributed to coal combustion, and POC from coal combustion was estimated to account for 12 % of the total PM_1 mass (Zhang et al., 2012b, 2013). Still from Beijing urban area, the primary organic aerosol (POA) from coal-combustion was also found to be most important fraction of total POA, and accounted ∼ 33 % of total organic aerosol (Sun et al., 2014). Biomass burning and motor vehicle are the two other major sources for POC (Cao et al., 2010; Lu et al., 2011), and their contribution to OC will be discussed in Sect. 3.4.

The mass fractions of nitrate and ammonium normally were around 5 to 10 and 3 to 7 %, respectively. The mass fraction of nitrate was less than 5 % in rural northwest China (Gaolanshan and Dunhung) and that of ammonium was less than 3 % in rural northwest China, urban Haze Region V (Panyu), and urban Haze Region I (Dalian) (Fig. 2b). The percentage of nitrate and ammonium in 2013 had no significant differences with those in 2006 and 2007 (Zhang et al., 2013). Comparing the nitrate mass in PM_{10} among the stations within Haze Region II in 2013 (Table 2), the concentrations in urban Beijing (~ $20\,\mu g\,m^{-3}$, from 2009 data because no data was obtained in 2013) were not higher than those in other stations (19 to $22\,\mu g\,m^{-3}$ for Zhengzhou, Gucheng, and XiAn). However, the contribution from motor vehicle emission is the largest in BIV (NBS-Beijing, 2013). This result shows that nitrate over the region does not only originate from motor vehicle emission but also from coal combustion. Even in BIV, about 28 % of the emission amount of NO_x can still be attributed to coal combustion. In other areas in China, about 50 % of nitrate mass can be attributed to coal combustion (Cao et al., 2010). Globally, NO_x is mainly derived from natural sources. However, in urban areas, NO_x mainly comes from anthropogenic activities such as oil and coal combustion. Given the rapid development of China's economy in recent years, the amount of gasoline and diesel oil consumption has significantly increased over the past few years (Lu et al., 2011), even if the Chinese government started promoting the "low nitrogen combustion technology" for denaturalization in power generation since 2012. The installation capacity reached only around 70 % until the middle of 2013, except in BIV (meeting communication), which can probably explain the high nitrate concentration in HBP.

In most areas in China (Fig. 2b), EC normally accounts for 3 to 4 % of aerosol mass, with less than 2 % in rural northwest China (Fig. 2b); this result is also similar to the data obtained from 2006 to 2007 (Zhang et al., 2013). The EC has similar sources with POC (Cao et al., 2010), and is not a major chemical fraction in aerosol particles over China.

Almost similar concentrations were found for each chemical component in aerosol particle with diameters less than 10 µm (PM_{10}) and less than 2.5 ($PM_{2.5}$) were observed in urban Beijing, respectively (Table 2). These results provide further evidence that the secondary aerosol particle (sulfate, nitrate, ammonium, and SOC) and particles from combustion processes (EC and POC) are present in particles with a diameter of $< 2.5\,\mu m$.

3.3 Changes of annual mean concentration of chemical components

Table 2 provides the annual averaged daily concentrations for PM_{10} of major chemical components in six major haze areas of China from 2012 to 2013. In the Gucheng station (Haze Region II), the annual mean concentrations of most chemical components had no significant difference between 2013 and 2012, except OC with an increase of $\sim 10\,\mu g\,m^{-3}$ in 2013. This result indicates that no significant difference was observed in emission between the two years. About 37.5 and 36.2 billion tons of standard coal were used for energy consumption in 2013 and 2012 (NBS-China, 2014), respectively, and the difference is not that high. The mass of mineral aerosol in 2013 was even bit lower than that in 2012, resulting in a relatively lower yearly mean PM_{10} concentration in 2013 but was unexpectedly associated with the occurrence of persistent heavy haze-fog events in the winter of 2013. This event did not occur in 2012. As such, this difference was the subject of studies because no significant changes were observed in the emission. Gucheng station is located in a rapidly urbanized area of Baoding city, Hebei province, which is the closest city to Beijing (about 140 km southwest). Zhengzhou, XiAn, and Beijing are all within the Haze Region II. The annual concentration levels of chemical components were not significantly different between 2013 and 2012.

A similar situation was also observed in stations such as LinAn, Jinsha, and Changde in Haze Region III (YRD area), Panyu in Haze Region V (PRD area), Chengdu in Haze Region VI (SCB area), Dalian in Haze Region I (N. E. China), and Gaolianshan and Dunhuang in Haze Region IX (N. W. China) (Table 2). As such, no evident annual concentration differences were observed in 2012 and 2013 in terms of the major chemical components, especially those associated with fine particles such as SO_4^{2-}, OC, NO_3^-, NH_4^+, and EC.

Comparing the annual averaged concentrations, the annual mean of most chemical components in 2013 are even lower than those from 2006 to 2007 (Zhang et al., 2012a). A survey of the main aerosol chemical components shows a wide spatial variability and higher concentrations for all aerosol components in aerosol mass concentration in the same stations from 2006 and 2007. For these annual mean concentrations, large decreases were observed in 2013 relative to the values from 2006 to 2007 in Gucheng station for various major chemical species, especially for SO_4^{2-}, NH_4^+, and NO_3^- with 2006 to 2007 to 2013 ratios of 1.5, 1.5, and 1.2, respectively. The only component whose concentration increased in 2013 was OC. The reason will be discussed in the next section. For EC and mineral aerosol, their concentrations exhibited no evident changes. The same result was observed for stations (Zhengzhou, XiAn) within the same haze region (II), where the concentrations of most chemical components, except for OC and mineral aerosol, were all lower in 2013 relative to those from 2006 to 2007. Moreover, the final PM_{10} concentration in 2013 was also lower than that from 2006 to 2007.

3.4 Occurrence of haze-fog event in January of 2013 as opposed to 2012 in Gucheng in Haze Region II as an example

3.4.1 Winter concentration and year-long aerosol pollution

The typical seasonal patterns in various aerosol components in China are summarized by (Zhang et al., 2012a), where the maximum concentrations of most aerosol chemical components were observed in winter, whereas that of mineral aerosol was observed in spring. In addition to the regular seasonal maximum, secondary peaks were found for sulfate and ammonium during the summer and for OC and EC during June and October. The general changing patterns of various chemical components were also true in Gucheng at this study (Fig. 3 – left panel). The OC concentration from late autumn to winter season was normally 2 to 4 times higher than those in summer, and the concentration during winter continuously declined from 2006 to 2009 and then increased from 2010 to 2013. This result can also be seen in the linear trend of wintertime concentration from 2010 to 2013 in Fig. 3. The averaged OC concentration in January of 2013 even reached $\sim 145\,\mu g\,m^{-3}$, which is a ~ 2.2 time higher than that in 2010. A similar situation was also observed for EC, SO_4^{2-}, NO_3^-, NH_4^+, and PM_{10}.

Although the annual mean concentration had no evident changes, the winter concentration of PM_{10} was higher by at least 25 % in 2013 than in the winter of 2012, whereas the winter concentrations of SO_4^{2-} and NH_4^+ in 2013 even increased by a factor of 1 or near 1 relative to that in to 2012, and the OC concentration increased by ~ 50 %. All these increases resulted in the heavy and persistent haze-fog event in January of 2013.

Based on the OC concentration histogram in Fig. 3 (right panel), the OC concentration is usually 15 $\mu g\,m^{-3}$, which can be considered as the regurlarly-observed background concentration in Haze Region II. A peak concentration of 55 $\mu g\,m^{-3}$ can be considered as the maximum wintertime mass of OC. As discussed in Sect. 3.2, the increased value of OC concentration during the winter can be partially attributed to scattered and central centralized coal combustion during the heating season. Aside from this, the increased OC concentration during the winter was also highly correlated with biomass fuel burning in Gucheng, Baoding city, Hebei province in the south of Beijing during the winter. The OC/EC ratio was 4.6 for Gucheng in the winter of 2013 and ranged from 4.1 to 4.5 during wintertime in other years. This group "Gucheng" ratio (4.1 to 4.6) is between the ratio of biomass fuel combustion (3.3) and open biomass burning (8.9 in winter, 8.0 in spring, 5.6 in summer, and 5.9 in autumn) based on the emission inventory (Cao et al., 2006, 2010), but is much higher than the ratio of coal combustion (2.0), gasoline (1.4), and diesel oil (3.0), as well as the normal value of 3.1 to 3.9 for ambient aerosol in urban areas in China (Zhang et al., 2008). Thus, biomass fuel burning was identified to be another main source for the increase in OC concentration during winter in these areas in the past few years. Baoding (Gucheng station located) is the nearest city in Hebei province to Beijing and has a population of about 11 million, in which ~ 80 % are rural dwellers living in more than 600 villages of 27 counties. Even in urban areas with more than 2 million inhabitants, the proportion of central heating during winter in Baoding is less than 40 %. In the village and country, large amounts of biomass and scattered coal were burned during winter for heating. During summer, the OC/EC ratios ranged from 1.6 to 3.0 from 2008 to 2012 and 2.6 to 3.4 from 2006 to

2007 (Zhang et al., 2008). As such, the contribution of gasoline and diesel combustion during summer to the OC concentration is high, which is evidently different during the winter.

The change in EC is similar to that in OC, and its background concentration is around 5 $\mu g\,m^{-3}$. In winter, the value is about 21 $\mu g\,m^{-3}$.

In Fig. 2b, sulfate, similar to OC, accounted for a large fraction (~ 12 %) of PM_{10} in 2013 in Gucheng, and its seasonal variation pattern is similar to the general trend in other areas of China (Zhang et al., 2012a) with the maximum concentrations found during winter, and secondary peaks during summer (Fig. 3 – left panel). The histogram analysis for sulfate (Fig. 3 – right panel) also shows two peak values of 43 and 33 $\mu g\,m^{-3}$, which may represent the peak concentrations in winter and summer, respectively. Another peak at 21 $\mu g\,m^{-3}$ may represent the background value. Based on the winter sulfate concentration from 2010 to 2013, a slight increase in SO_4^{2-} concentration was observed from linear fitting of SO_4^{2-} in Fig. 3 (lift panel), particularly in January of 2013. A peak at 56 $\mu g\,m^{-3}$ was observed, thereby indicating that the sulfate probably originated from scattered coal combustion and central heating involving the use of coal in Gucheng because the major emission sources for SO_2, i.e., coal power plant and industrial manufacturing processes, would be no extra increase during winter. In China, half of coal is used for power generation. About three quarters of another half are used in industrial manufacturing processes, mainly in steel mills, chemical plants, and glass and cement plants, and a quarter of this half can be attributed to scattered coal combustion for winter heating (Cao et al., 2010). Only this part caused the increase during winter. The emissions of scattered coal combustion were those from smaller heating boilers (less than 40 tons) and those of coal burning were from scattered residential households. All sulfate data fitting (not just based on wintertime data) still shows the decreasing trend from 2010 to 2013 (–0.07 slope for linear fitting, data omitted), Thus, desulphurization processes in power plant, which have been carried out 2000 in China, might cause these decreases.

Similar to sulfate, nitrate concentration was also higher in winter relative to other seasons, and an increasing trend during winter was observed from 2010 to 2013 with less significant seasonal variations relative to OC and EC (Fig. 3 – left panel). Given that the main sources of NO_x emission, i.e., coal combustion from coal power plants, industrial manufacturing processes, fuel burning from motor-vehicle, and natural gas burning (Göke et al., 2014), are relatively the same for all four seasons, the contribution of scattered coal heating or central heating boilers without denitrification devices to the increase of NO_3^- concentration during winter cannot be ignored. The lower height of the plenary boundary during the winter is another reason for the high concentration during winter. If one just compares the winter data, the effect would be eliminated. This is, of couse, an important aspect to determine the impact of meteorological factors on pollution and will be discussed in the next section by using PLAM. Based on the NO_3^- histogram result (Fig. 3 – right panel), the regional background and winter peak concentrations are around 12 and 28 $\mu g\,m^{-3}$, respectively. Unlike in sulfate, the linear fit by using all nitrate data still showed an increasing trend for NO_3^- (Fig. 3 – left panel), thereby showing that the denitrification in power plants since 2012 had no obvious effect in the increase in NO_3^- concentration.

Of the anions, SO_4^{2-} and NO_3^- are dominant species contributing to aerosol acidities, both of which are highly correlated with NH_4^+ in Gucheng (Zhang et al., 2012a). The median ratio of the observed mole number of NH_4^+ and capable molecules for neutralizing this substance from SO_4^{2-} and NO_3^- was approximately 0.70 from 2006 to 2013, thereby suggesting that excess overbalanced anion can sufficiently neutralize NH_4^+ in Haze Region II. The change in NH_4^+ concentration since 2010 was similar to that of NO_3^-, with the same tendency to increase during winter (Fig. 3 – left panel). The frequency distribution was also similar to that of NO_3^- bit different with that of SO_4^{2-} (Fig. 3 – right panel). The frequency distribution analyses of NH_4^+ concentration also showed that the background and winter concentrations were 7.5 and 23 $\mu g\,m^{-3}$, respectively (Fig. 3 – right panel). Both values are much higher in the HBP area than in other regions, which imply that the major sources of NH_4^+ are located in the HBP. Waste and coal consumption account for ~ 67 to 85 % of the total NH_3 emissions, of which human and poultry wastes as well as coal combustion from industry, commercial, and residential usage are the major contributors in urban areas (Cao et al., 2010). In rural areas, another source of ammonia emission is agricultural activities, which account for ~ 14 to 28 % of the total NH_3 emission, with nitrogen fertilizer as the major contributor (Cao et al., 2010).

In Fig. 3 – left panel, the linear trend of winter mineral aerosol concentration shows almost no change from 2010 to 2013, thereby indicating that the change in PM_{10} in these years was mainly attributed to the changes in fine aerosol particle concentrations. The histogram analysis of the mineral suggests that a high regional background loading of 90 $\mu g\,m^{-3}$ was observed in the Haze Region II, which not only caused by sand-dust-storm dust, urban fugitive dust, but also coal ash that is highly related with the large amount of coal combustion activities in this area. The winter concentration of mineral aerosol is around 130 $\mu g\,m^{-3}$ (Fig. 2 – right panel).

3.4.2 Contribution of specific meteorological condition to the wintertime PM_{10} changes

The PM_{10} concentration increased by about 25 % in January of 2013 compared with that in 2012. The specific meteorological conditions that are highly related with aerosol pollution (parameterized as an index called "PLAM") also increased by ~ 15 % at the same period. Given that the pollutant emissions did not significantly change from 2012 to 2013 (NBS-China, 2014), which was not enough to cause a significant increase of 25 %, about 60 % of this 25 % increase in PM_{10} concentration can thus be considered as the contribution of worsening meteorological conditions because PLAM has been confirmed to be linearly related with PM_{10} concentration (Wang et al., 2012).

The comparison of averaged PM_{10} concentration between January 2013 and January 2010 also showed that the mean value in 2013 was 1.2 times higher than that in 2010, whereas the PLAM index increased to about 35 % in 2013 compared with that in 2010. Given the linear relation between PLAM and PM_{10} (Wang et al., 2012), about 28 % of the 1.2 times increase in PM_{10} can be approximately regarded as the contribution from worsening meteorological conditions since 2010. Based on the changes in mean mass of various chemical components between January 2010 and January 2013 and by multiplying these by the proportion of each component of PM_{10} in 2013 (Fig. 2b), about 20, 41, 18, 16, 2.0, and −5.0 % of the increase in PM_{10} in 2013 relative to 2010 can be attributed to SO_4^{2-}, OC, NO_3^-, NH_4^+, EC, and mineral, respectively. The other components accounted for about ∼ 9 % of this increase in PM_{10} concentration between 2010 and 2013. OC contributed the largest percent of the increase in PM_{10} concentration from 2010 to 2013.

3.5 Changes in the chemical components of PM_{10} in other major haze areas in China

3.5.1 Haze Region III (Yangtze River Delta (YRD) area) in China

Although the winter concentrations of particular aerosol chemical components, such as OC, NO_3^-, and NH_4^+, continuously increased since 2010 in Haze Region III (LinAn) (Fig. 4 – left panel), the increase in amplitude was much smaller than that of HBP. The winter concentration of EC and dust slightly decreased and that of sulfate did not significantly change from 2010 to 2013. Thus, PM_{10} concentration remained unchanged since 2010, which was very similar to the change in wintertime PLAM since 2010 in the same area. This result implies the important effect of meteorological condition on aerosol pollution. In general, the pollution-meteorological condition worsened from 2006 to 2010 in Haze Region III (LinAn) and remained almost unchanged from 2010 to 2013 with a slight decrease in 2011 (Fig. 4 – left panel-upper part).

The regional background concentrations of SO_4^{2-}, OC, NO_3^-, NH_4^+, EC, and mineral dust are normally 17, 11, 6, 6, 3, and 25 $\mu g\,m^{-3}$, respectively, which are about 60 to 80 % of the HPB level (Fig. 4 – right panel). The corresponding winter values are normally 33, 22, 15, 10, 5, and 65 $\mu g\,m^{-3}$, respectively. The winter values were still more than 1 times higher than the annual background concentration, but the concentrations are much smaller than in HBP, thereby suggesting the weak influence of winter heating in the YRD area. Winter heating is not legally imposed in the southern parts of China. However, coal-fired heating during winter is still practiced in this area, which can increase the mineral content to 65 µg m^{-3} during winter from the normal value of 25 µg m^{-3}. The increased wintertime mineral concentration is most likely caused by coal ash, whereas other fugitive dust, such as dust from sand and dust storm events, construction sites, and unpaved roads, would cause a significant increase during winter. Unlike in HBP, the proportion of sulfate ($\sim$ 19 % of PM_{10}) is much higher than the OC fraction (13 % of PM_{10}).

The winter OC/EC ratio was 3.7 with a range of 2.7 to 5.3 from 2006 to 2013 in Haze Region III (LinAn), and a high value of $\sim$ 4.0 was observed from 2012 to 2013. These values are similar those from biomass fuel combustion (Cao et al., 2010), thereby suggesting that the influence of biomass burning for heating was also observed in the YRD area during winter.

3.5.2 Haze Region V (Pearl River Delta (PRD) area) in China

The pollution-meteorological conditions during wintertime were much better in Haze Region V (Panyu) in the PRD area than that in the HBP, with PLAM values ranging from 60 to 90 from 2010 to 2013 (corresponding values of 110 to 150 in HPB; $\sim$ 120 to 125 in YRD) and are associated with a declining trend (Fig. 5-left panel-upper part). This decrease in PLAM was very similar to the decreased trend of PM_{10}, thereby implying the effect of meteorological factors on the change in PM. In Fig. 5, almost all chemical components presented a decreasing since 2010, except for nitrate. In addition to the reduced emission in YRD with emphasis on coal combustion sources, the decrease in the concentrations of major chemical components and PM_{10} can also be partially attributed to improved meteorological conditions since 2010. The proportion of coal in primary energy consumption decreased to 49 % in 2013 in Guangzhou. The corresponding number is 60 % in 2004 (meeting communication).

The regional background concentrations of SO_4^{2-}, OC, NO_3^-, NH_4^+, EC, and mineral dust in this region are 17, 13, 9, 7, 3.5, and 25 µg m^{-3}, respectively, which are similar to the values in YRD. The corresponding winter values are 33, 22, 15, 9, 6.7, and 70 µg m^{-3} for SO_4^{2-}, OC, NO_3^-, NH_4^+, EC, and mineral, respectively. The difference between the winter and background concentrations in other season in the PRD area is very similar to those in the YRD area.

The winter OC/EC ratio in Haze Region V (Panyu) is 0.79 with a range of 0.25 to 2.9 from 2006 to 2013, which is close to the value of 1.4 for gasoline (Cao et al., 2010). Thus, different sources were noted in the HBP area for OC and EC with less biomass burning contribution. In January of 2006, 2008, and 2009, the OC/EC ratios were within the range of 2.4 to 2.9, which were very similar to the fossil fuel combustion (2.0) and diesel oil (3.0) (Cao et al., 2010). As such, emission had an evident effect in reducing the contribution of coal combustion and diesel vehicles in Guangzhou. After 2010, the winter ratio of OC and EC were within 0.3 to 0.5.

3.5.3 Haze Region VI (Si Chuan Basin (SCB) area) in China

Based on the monthly changes in the various chemical components and PM_{10} in Haze Region VI (Chengdu) (Fig. 5 – left panel), the wintertime mass of various chemical components generally had peak values from 2006 to 2013. However, in particular years, this kind of situation was not particularly evident. These results suggest that the wintertime heating season had an effect on the chemical composition in the SCB area. Specifically, the mass of mineral aerosol was found to have an evident peak in winter, which is different from other areas. As such, the influences of coal-ash contribution were observed. The significant increase in the concentration during winter was not evident for sulfate relative to other chemical species, such as EC and nitrate, especially after 2010, because another period had existed in the summer where the values were at their maximum. Moreover, the decreasing trend of sulfate in January from 2010 to 2013 shows the effect of desulfurization in this area. The opposite behavior was observed for nitrate during the same period, showing no obvious denitrification effect of power generation plants. During winter, PLAM decreased from 2006 to 2009 and remained at a similar level at ~ 130 from 2010 to 2013. However, the value was low in 2011, thereby showing that the effect of bad weather on aerosol pollution is medium in the SCB area (Fig. 5-left panel-upper part).

The background concentrations of SO_4^{2-}, OC, NO_3^-, NH_4^+, EC, and mineral dust in this region are 23, 22, 9, 7, 5, and 65 $\mu g\,m^{-3}$, respectively, which are similar to the HBP value, with slightly higher masses for SO_4^{2-} and OC and slightly lower values for NO_3^- and mineral dust. The corresponding winter values are 43, 47, 23, 18, 14, and 145 $\mu g\,m^{-3}$. The difference between the winter and background concentrations in the SCB area is very similar to that in the HBP area, thereby showing the relatively polluted condition in this area.

In general, two values of OC/EC were obtained: ~ 3.1 in December to January and ~ 0.41 in February. The higher OC/EC ratio is quite similar to biomass fuel combustion (3.3), and the lower value is close to gasoline (1.4) (Cao et al., 2010). These results suggest the contributions of biomass burning for heating during winter in the SCB area, and the contribution from motor vehicle was also observed. The low OC/EC ratio during winter is also similar to most values of OC/EC during other seasons, thereby showing the strong influences of motor vehicle to OC and EC in this area.

4 Summary

On the basis of mass concentration of sulfate, OC, nitrate, ammonium, EC, and mineral dust from 24 h aerosol particle (PM_{10}) collected from various CAWNET stations from 2006 to 2013, the change in these major water-soluble constituents, carbonaceous species, mineral aerosol and PM_{10} since 2006 and the contribution of meteorological condition were investigated in this study. The mass concentration and comparison of the chemical components in major haze regions of China were also provided with details for 2012 and 2013 in particular, in hope to strengthen the understanding of the growing haze-fog over the years in China. Moreover, this study can also serve as a basis in chemical composition aspect for further evaluation the effect of implementation of various pollution control countermeasures after 2013, called "atmospheric pollution prevention and control of the ten measures of China" by Chinese government. This investigation also provides the inputs and validation of haze-fog forecasting system that used a lot of near-real time (NRT) data.

The major findings of this study can be summarized as follows:

- During 2013, the mineral aerosol was found still to be the largest component of PM_{10} in almost all stations in different haze areas, thereby showing the high "dust" characteristics in aerosol pollution of China, in which the contribution of coal-ash should not be ignored. Thus, a high mineral concentration was observed even at southern part of the urban areas in China. The high regional background loading of 90 $\mu g\,m^{-3}$ in mineral aerosol was observed in the Haze Region II, which not only caused by sand-dust-storm dust, urban fugitive dust, but also coal ash that is highly related with the large amount of coal combustion activities in this area. The winter concentration of mineral aerosol is around 130 $\mu g\,m^{-3}$. Sulphate contributed the second, and the first large anthropogenic, mass fraction to the atmospheric aerosol (i.e., 12 to 25 %) in most of areas of China except rural northwest China. At stations of Gucheng, XiAn and Panyu, the sulphate fraction were bit lower than OC and ranked the third, but still with a percentages of 9 to 16 %. OC normally ranked the third and accounted for about 7 to 19 % by mass, with high proportions in Gucheng and Panyu. The mass fractions of nitrate and ammonium were normally around 5 to 10 and 3 to 7 %, while in most areas of China, elemental carbon represented 2 to 4 %. All these percentage are similar with the results of 2006 and 2007 (Zhang et al., 2012a). More than 50 % of primary OC and 28 to 50 % nitrate mass were attributed to coal-combustion. In the stations of Gucheng, Zhengzhou and XiAn in HBP, the nitrate concentrations are all higher than or close to that in Beijing that has the largest number of motor vehicles within the Haze

Region II. The result suggests that coal-combustion also has an important contribution to the increased nitrate concentration in this area. NH_4^+ concentration are much higher in HBP than in other regions, with the background and winter concentrations of 7.5 and 23 $\mu g\,m^{-3}$, respectively, which imply that the major sources of NH_4^+ are located in the HBP. Agricultural activity is the most important source of ammonium.

- Excessive amount of unclean energy-consumption was the most fundamental reason for the increased severity of haze and fog events in China, in which coal-combustion was still the largest anthropogenic source for aerosol pollution in various areas of China in 2013. The proportion of each chemical component of PM_{10} had no evident changes from 2006 to 2013, which also shows that the sources for aerosol particles did not significantly change from 2006 to 2013.

- Wintertime mass concentrations of aerosol chemical components and PM_{10} are more important than annual mean value in evaluating of aerosol pollution for a year. In the HBP area, the winter concentration in various components normally exhibited a decline during 2006 to 2010 (considered as the first phase for the pollution change during 2006–2013), and then rose till 2013 (called second phase). The wintertime PM_{10} was 1.2 times higher in 2013 than it in 2010, in which ~ 28 % of the increase in PM_{10} concentration from 2010 to 2013 can be attributed to the worsening specific meteorological conditions based on the PLAM results. The increased sulfate, OC, nitrate, ammonium, EC and mineral dust contributed about 20, 41, 18, 16, 2.0, and −5.0 % to the increased PM_{10} concentration from 2010 to 2013, and ~ 9 % of the increased PM_{10} concentration can be attributable to other components, including trace metal, other water soluble species, other organic matter, and biogenic aerosol. The winter concentrations were usually around 43, 55, 28, 23, 21 and 130 $\mu g\,m^{-3}$ for SO_4^{2-}, OC, NO_3^-, NH_4^+, EC and mineral dust, respectively, which were about 2–4 factors higher than the background masses, with corresponding values of 20, 15, 12, 7.5, 5 and 90 $\mu g\,m^{-3}$ in the HBP area.

- Given the ~ 25 % increase in PM_{10} concentration in January of 2013, relative to 2012 in the HBP area, while the winter values of SO_4^{2-} and NH_4^+ concentrations in 2013 even increased by 1 or near 1 factor in 2013, relative to 2012. The OC concentration increased by ~ 50 %. All these resulted in persistent haze-fog event in January of 2013, which did not happen in the winter of 2012. About ~ 60 % of this increment can be attributable to worsening meteorological conditions. The APEC summit period (8–10 November 2014) was associated with bad meteorological conditions with ~ 100 to 120 of PLAM at Beijing, ~ 35 % reduction of pollutant emission in the BIV area by various control measures. This ~ 35 % cut resulted in good air quality, and was called "APEC blue" in media (all the details will be introduced in a companioned paper separately). From the fact of increment of ~ 25 % pollutants in the HBP area resulted in persistent haze-fog event in winter 2013, and ~ 35 % cutting derived in APEC Blue in 2014 winter, one could approximately estimates that there will be no frequent persistent haze-fog event induced by aerosol pollution if ~ one third of pollutant emission can be reduced on the basis of winter emission level of 2013 in BIV. The ~ one-third reduction of 2013 winter emission might be considered as the upper limit of capacity of aerosol pollution in this area.

- OC contributed the largest in the increase in PM_{10} concentration during winter from 2010 to 2013 in the HBP area, in which the contribution from biomass fuel burning for heating was identified in addition to the contribution from the scattered and central coal-combustion for heating. The phenomenon was also found in YRD area and SCB but not in PRD area, where the contribution from the coal-combustion to various chemical components was noted before 2009, but after 2010, the contributions from motor vehicle increased.

- All sulfate data fitting from 2010 to 2013 shows a decreasing trend in the HBP area that is opposite of the fitting when only wintertime data are used, thereby reflecting the effect of power plant desulphurization since 2002 in China. This is also true for PRD and SCB areas, but almost no change in the YRD area. Unlike in sulfate, the linear fit using all season nitrate data in the four major haze regions still showed an increasing trend from 2010 to 2013, thereby partially showing the lack of effect of power plant denitrification. Since large-scale caring on power plant denitrification started in 2012 in China, the effect of desulphurization is not yet fully expressed. Of course the increased number of motor vehicle and the burning of more natural gas also contributed to the increase in nitrate concentration over these years.

- In Haze Region III (YRD area), although there were some changes in different chemical components between 2010–2013, the PM_{10} concentrations in winter season remained unchanged and is associated with similar changes in PLAM. The regional background concentrations of SO_4^{2-}, OC, NO_3^-, NH_4^+, EC and mineral dust are normally 17, 11, 6, 6, 3 and 25 $\mu g\,m^{-3}$, respectively. The corresponding winter high values are normally 33, 22, 15, 10, 5 and 65 $\mu g\,m^{-3}$ for each of them. The weak influence of winter heating was identified in this area.

- In Haze Region V (PRD area), the pollution-meteorological conditions during winter were much better than that in the HBP, and continually getting better from 2010 to 2013. This improvement is associated with a declining in almost all chemical components and PM_{10} during winter, with less change for nitrate. This trend is the opposite of that in HBP. Within the same Haze Region V, nitrate mass was a factor higher in Panyu of Guangdong province than in Nanjing of Guangxi province, thereby showing a relatively larger influence of motor vehicle and natural gas burning on nitrate concentration in Panyu compared with that in Nanjing. Similar to the mass and difference between winter and normal conditions in the YRD area, the regularly-observed background concentrations of SO_4^{2-}, OC, NO_3^-, NH_4^+ and EC are normally 17, 13, 9, 7, 3.5 and 25 $\mu g\,m^{-3}$, respectively, corresponding with winter high values of 33, 22, 15, 9, 6.7 and 70 $\mu g\,m^{-3}$ for each of them, respectively.

- In Haze Region VI (SCB area), the background and higher concentrations of chemical components and PM_{10} in winter were all similar to those of the HBP, with background masses of 23, 22, 9, 7, 5 and 65 $\mu g\,m^{-3}$ for SO_4^{2-}, OC, NO_3^-, NH_4^+, EC and mineral dust, respectively, and the corresponding mass of winter high masses of 43, 47, 23, 18, 14 and 145 $\mu g\,m^{-3}$. During winter, the contributions of biomass fuel burning from heating to OC and EC were also identified in this area, and the contribution from motor vehicles also observed in other part of wintertime and other season. The change in chemical components in January and the associated changes in PLAM in the SCB area were similar to those in the YRD area, with a slight change in winter, 130 of PLAM, for aerosol pollution from 2010 to 2013.

- Evidence of comparisons for the chemical components in PM_{10} and $PM_{2.5}$ in Beijing suggests that the secondary aerosol particle (sulfate, nitrate, ammonium, SOC), and particles from combustion (EC and POA) are almost associated with the particles with diameters smaller than 2.5. The measurement of PM_{10} from monitoring or filter analysis can provide information that covers all kinds of information related to chemical components of $PM_{2.5}$ and also includes information about mineral dust, especially those with diameters between 2.5 and 10 um, which can fully reflect the problems of aerosol pollution in China.

Acknowledgements. This research was supported by grants from National Key Project of Basic Research (2011CB403401) and Specific Team Fund of the Jiangsu Collaborative Innovation Center for Climate Change. We sincerely thank the support of aerosol sampling from CAWNET staffs of CMA.

References

Boucher, O., Randall, D., Artaxo, P., Bretherton, C., Feingold, G., Forster, P., Kerminen, V.-M., Kondo, Y., Liao, H., Lohmann, U., Rasch, P., Satheesh, S. K., Sherwood, S., Stevens, B., and Zhang, X. Y.: Clouds and aerosols, in: Climate Change 2013: the Physical Science Basis, contribution of Working Group I to the Fifth Assessment Report of the Intergovernmental Panel on Climate Change, edited by: Stocker, T. F., Qin, D., Plattner, G.-K., Tignor, M., Allen, S. K., Boschung, J., Nauels, A., Xia, Y., Bex, V., and Midgley, P. M., Cambridge University Press, New York, 614–620, 2013.

Cao, G., Zhang, X., and Zheng, F.: Inventory of black carbon and organic carbon emissions from china, Atmos. Environ., 40, 6516–6527, 2006.

Cao, G. L., An, X. Q., Zhou, C. H., Ren, Y. Q., and Tu, J.: Emission inventory of air pollutants in china, China Environmental Science, 30, 900–906, 2010.

Chow, J. C., Watson, J. G., Pritchett, L. C., Pierson, W. R., Frazier, C. A., and Purcell, R. G.: The dri thermal/optical reflectance carbon analysis system: description, evaluation and applications in US air quality studies, Atmos. Environ., 27A, 1185–1201, 1993.

Chow, J. C., Watson, J. G., Chen, L.-W. A., Arnott, W. P., Moosmüller, H., and Fung, K. K.: Equivalence of elemental carbon by thermal/optical reflectance and transmittance with different temperature protocols, Environ. Sci. Technol., 38, 4414–4422, 2004.

Donkelaar, A. V. and Villeneuve, P. J.: Global estimates of ambient fine particulate matter concentrations from satellite-based aerosol optical depth: development and application, Environ. Health Persp., 118, 847–855, 2010.

Forster, P., Ramaswamy, V., Artaxo, P., Berntsen, T., Betts, R., Fahey, D. W., Haywood, J., Lean, J., Lowe, D. C., Myhre, G., Nganga, J., Prinn, R., Raga, G., Schulz, M., and Dorland, R. V.: Changes in atmospheric constituents and in radiative forcing [m]//ipcc, in: Climate Change 2007: the Physical Science Basis, contribution of Working Group I to the Fourth Assessment Report of the Intergovernmental Panel on Climate Change, edited by: Solomon, S., Qin, D., Manning, M., Chen, Z., Marquis, M., Averyt, K. B., Tignor, M., and Miller, H. L., Cambridge University Press, Cambridge, UK and New York, USA, 153–171, 2007.

Gao, S., Wang, X., and Zhou, Y.: Generation of generalized moist potential vorticity in a frictionless and moist adiabatic flow, Geophys. Res. Lett., 31, L12113, doi:10.1029/2003GL019152, 2004.

Göke, S., Schimek, S., Terhaar, S., Reichel, T., Göckeler, K., Krüger, O., Fleck, J., Griebel, P., and Paschereit, C. O.: Influence of pressure and steam dilution on NO_x and CO emissions in a premixed natural gas flame, J. Eng. Gas Turb. Power, 136, GTP-14-1050, doi:10.1115/1.4026942, 2014.

Guo, S., Hu, M., Zamora, M. L., Peng, J., Shang, D., Zheng, J., Du, Z., Wu, Z., Shao, M., and Zeng, L.: Elucidating severe urban haze formation in china, P. Natl. Acad. Sci. USA, 111, 17373–17378, 2014.

He, K., Yang, F., Ma, Y., Zhang, Q., Yao, X., Chan, C. K., Cadle, S., Chan, T., and Mulawa, P.: The characteristics of $PM_{2.5}$ in Beijing, China, Atmos. Environ., 35, 4959–4970, 2001.

Hu, M., He, L. Y., Zhang, Y. H., Wang, M., Pyo Kim, Y., and Moon, K. C.: Seasonal variation of ionic species in fine particles at qingdao, Atmos. Environ., 36, 5853–5859, 2002.

Huang, R.-J., Zhang, Y., Bozzetti, C., Ho, K.-F., Cao, J.-J., Han, Y., Daellenbach, K. R., Slowik, J. G., Platt, S. M., and Canonaco, F.: High secondary aerosol contribution to particulate pollution during haze events in china, Nature, 514, 218–222, 2014.

Johnson, A. B. and Baker, D. G.: Climatology of diffusion potential classes for Minneapolis – St. Paul, J. Appl. Meteorol., 36, 1620–1628, 1997.

Li, J., Wang, G., Aggarwal, S. G., Huang, Y., Ren, Y., Zhou, B., Singh, K., Gupta, P. K., Cao, J., and Zhang, R.: Comparison of abundances, compositions and sources of elements, inorganic ions and organic compounds in atmospheric aerosols from Xi'an and New Delhi, two megacities in China and India, Sci. Total Environ., 476, 485–495, 2014.

Lu, Z., Zhang, Q., and Streets, D. G.: Sulfur dioxide and primary carbonaceous aerosol emissions in China and India, 1996–2010, Atmos. Chem. Phys., 11, 9839–9864, doi:10.5194/acp-11-9839-2011, 2011.

NBS-Beijing: Beijing Statistical Yearbook, Beijing, China Statistical Press, 2013.

NBS-China: China Statistical Yearbook, Beijing, China Statistical Press, 2014.

Pang, X., Mu, Y., Lee, X., Zhang, Y., and Xu, Z.: Influences of characteristic meteorological conditions on atmospheric carbonyls in Beijing, China, Atmos. Res., 93, 913–919, 2009.

Pérez, C., Nickovic, S., Pejanovic, G., Baldasano, J. M., and Özsoy, E.: Interactive dust-radiation modeling: a step to improve weather forecasts, J. Geophys. Res., 111, 1–17, 2006.

Seinfeld, J. H. and Pandis, S. N.: Atmospherical Chemistry and Physics: from Air Pollution to Climate Change, John Wiley & Sons, Inc., New York, 1997.

Sui, K., Wang, Z., Yang, J., Xie, F.-Y., and Zhao, Y.: Beijing persistent PM_{10} pollution and its relationship with general meteorological features, Research of Environmental Sciences, 20, 77–82, 2007.

Sun, Y., Jiang, Q., Wang, Z., Fu, P., Li, J., Yang, T., and Yin, Y.: Investigation of the sources and evolution processes of severe haze pollution in Beijing in January 2013, J. Geophys. Res.-Atmos., 119, 4380–4398, 2014.

Twomey, S. J.: The influence of pollution on the shortwave albedo of clouds, J. Atmos. Sci., 34, 1149–1152, 1977.

Wang, H., Zhang, X. Y., Gong, S. L., Chen, Y., Shi, G. Y., and Li, W.: Radiative feedback of dust aerosols on the eastasian dust storms, J. Geophys. Res., 115, D23214, doi:10.1029/2009JD013430, 2010.

Wang, H., An, J., Shen, L., Zhu, B., Pan, C., Liu, Z., Liu, X., Duan, Q., Liu, X., and Wang, Y.: Mechanism for the formation and microphysical characteristics of submicron aerosol during heavy haze pollution episode in the Yangtze river delta, China, Sci. Total Environ., 490, 501–508, 2014.

Wang, J. Z., Gong, S., Zhang, X. Y., Yang, Y. Q., Hou, Q., Zhou, C., and Wang, Y.: A parameterized method for air-quality diagnosis and its applications, Advance of Meteorology, 2012, 1–10, doi:10.1155/2012/238589, 2012.

Wang, X., Chen, J., Sun, J., Li, W., Yang, L., Wen, L., Wang, W., Wang, X., Collett, J. L., and Shi, Y.: Severe haze episodes and seriously polluted fog water in Ji’nan, China, Sci. Total Environ., 493, 133–137, 2014.

Wang, Y. H., Liu, Z. R., Zhang, J. K., Hu, B., Ji, D. S., Yu, Y. C., and Wang, Y. S.: Aerosol physicochemical properties and implications for visibility during an intense haze episode during winter in Beijing, Atmos. Chem. Phys., 15, 3205–3215, doi:10.5194/acp-15-3205-2015, 2015.

Wang, Z., Li, J., Wang, Z., Yang, W., Tang, X., Ge, B., Yan, P., Zhu, L., Chen, X., and Chen, H.: Modeling study of regional severe hazes over mid-eastern China in January 2013 and its implications on pollution prevention and control, Sci. China Ser. D, 57, 3–13, 2014.

Watson, J.: Visibility: science and regulation, J. Air Waste Manage., 52, 628–713, 2002.

Xu, H., Bi, X.-H., Zheng, W.-W., Wu, J.-H., and Feng, Y.-C.: Particulate matter mass and chemical component concentrations over four chinese cities along the western pacific coast, Environ. Sci. Pollut. R., 22, 1–14, 2014.

Yang, Y.: A plam index forecast method for air quality of Beijing in summer, Journal of Applied Meteorological Science, 20, 649–655, 2009.

Yao, X., Chan, C. K., Fang, M., Cadle, S., Chan, T., Mulawa, P., He, K., and Ye, B.: The water-soluble ionic composition of $PM_{2.5}$ in Shanghai and Beijing, China, Atmos. Environ., 36, 4223–4234, 2002.

Ye, B., Ji, X., Yang, H., Yao, X., Chan, C. K., Cadle, S. H., Chan, T., and Mulawa, P. A.: Concentration and chemical composition of $PM_{2.5}$ in Shanghai for a 1 year period, Atmos. Environ., 37, 499–510, 2003.

Yin, L., Niu, Z., Chen, X., Chen, J., Xu, L., and Zhang, F.: Chemical compositions of $PM_{2.5}$ aerosol during haze periods in the mountainous city of Yong'an, China, J. Environ. Sci., 24, 1225–1233, 2012.

Zhang, X., Arimoto, R., An, Z., Chen, T., Zhu, G., and Wang, X.: Atmospheric trace elements over source regions for chinese dust: concentrations, sources and atmospheric deposition on the loess plateau, Atmos. Environ., 27, 2051–2067, 1993.

Zhang, X., Zhang, Y., and Cao, G.: Aerosol chemical compositions of beijing PM_1 and its control countermeasures, Journal of Applied Meteorological Science, 23, 257–264, 2012b, in Chinese with English abstract.

Zhang, X., Sun, J., Wang, Y., Li, W., Zhang, Q., Wang, W., Quan, J., Cao, G., Wang, J., Yang, Y., and Zhang, Y.: Factors contributing to haze and fog in China, Chinese Sci. Bull., 58, 1178–1187, doi:10.1360/972013-150, 2013.

Zhang, X. Y., Cao, J. J., Li, L. M., Arimoto, R., Cheng, Y., Huebert, B., and Wang, D.: Characterization of atmospheric aerosol over Xian in the south margin of the Loess Plateau, China, Atmos. Environ., 36, 4189–4199, 2002.

Zhang, X. Y., Gong, S. L., Shen, Z. X., Mei, F. M., Xi, X. X., Liu, L. C., Zhou, Z. J., Wang, D., Wang, Y. Q., and Cheng, Y.: Characterization of soil dust aerosol in China and its transport/distribution during 2001 ACE-Asia. 1. Network observations, J. Geophys. Res., 108, 8641–8650, doi:10.1029/2002JD002632, 2003.

Zhang, X. Y., Wang, Y. Q., Zhang, X. C., Guo, W., and Gong, S. L.: Carbonaceous aerosol composition over various regions of china during 2006, J. Geophys. Res., 113, D14111, doi:10.1029/2007JD009525, 2008.

Zhang, X. Y., Wang, Y. Q., Lin, W. L., Zhang, Y. M., Zhang, X. C., Gong, S., Zhao, P., Yang, Y. Q., Wang, J. Z., Hou, Q., Zhang, X. L., Che, H. Z., Guo, J. P., and Li, Y.: Changes of atmospheric composition and optical properties over Beijing 2008 olympic monitoring campaign, BAMS, November, 1634–1651, 2009.

Zhang, X. Y., Wang, Y. Q., Niu, T., Zhang, X. C., Gong, S. L., Zhang, Y. M., and Sun, J. Y.: Atmospheric aerosol compositions in China: spatial/temporal variability, chemical signature, regional haze distribution and comparisons with global aerosols, Atmos. Chem. Phys., 12, 779–799, doi:10.5194/acp-12-779-2012, 2012a.

Zhang, X. Y.: Characteristics of the chemical components of aerosol particles in the various regions over china, Acta Meteorol. Sin., 72, 1–11, doi:10.11676/qxxb2014.062, 2014, Chinese with English Abstract.

Table 1. Proportion change in major chemical components of PM_{10} at Gucheng.

	2006	2007	2008	2009	2010	2011	2012	2013
NO_3^-	0.10	0.07	0.04	0.07	0.06	0.06	0.09	0.10
SO_4^{2-}	0.16	0.14	0.09	0.12	0.13	0.13	0.10	0.12
NH_4^+	0.07	0.05	0.04	0.04	0.04	0.04	0.05	0.06
Mineral	0.32	0.36	0.42	0.48	0.52	0.32	0.44	0.40
OC	0.14	0.14	0.11	0.13	0.16	0.16	0.17	0.19
EC	0.05	0.04	0.03	0.04	0.04	0.04	0.04	0.04
Others	0.17	0.23	0.28	0.13	0.05	0.25	0.12	0.08

Table 2. Annual averaged daily concentrations ($\mu g\,m^{-3}$) for PM_{10}, chemical components in various regions of China during 2013 and 2012.

Stations	Type	Region	PM_{10}	Mineral	SO_4^{2-}	OC	NO_3^-	NH_4^+	EC	No.
Haze Region II (HBP)[a]										
Gucheng (GC)-2013	semi-urban	Province south of Beijing	196	74	21	45	17	10	10	52
2012-GC			203	84	20	36	17	10	8.1	101
Zhengzhou (ZZ)-2013	urban	Province south of Beijing	235	110	35	26	20	13	6.6	103
2012-ZZ			221	107	34	24	21	13	7.0	105
XiAn (XA)-2013	urban	Guanzhong Plain	293	138	31	34	20	11	11	81
2011-XA[b]			268	123	28	26	16	6.2	9.9	74
Beijing (BJ)-2009-PM_{10}[c]	urban	Haidian District of Beijing	174	nd	19	19	20	7.6	4.8	155
2009-$PM_{2.5}$[c]			126	nd	17	16	16	8.0	4.1	153
Haze Region III (YRD)										
LinAn (LA)-2013	rural	Yangtze River Delta regions	88	38	16	12	7.3	5.0	2.5	100
2012-LA			94	32	16	11	8.4	5.4	3.3	102
Jinsha (JS) -2013	rural	Lower reach of Yangtze River	78	28	19	8.5	5.8	5.4	2.2	52
2012-JS			86	33	21	8.7	6.5	5.7	2.2	52
Changde (TYS)- 2013	rural	Dongting and Buoyan lakes basin	72	16	18	10	6.1	6.1	2.0	82
2012-TYS			87	16	21	11	7.0	7.1	1.9	86
Haze Region V (PRD)										
Panyu (PY) -2013	urban	Pearl River Delta region	97	40	16	18	11	4.2	3.9	37
2012-PY			97	39	16	14	10	4.9	4.0	33
Nanning (NJ) -2013	urban	Pearl River Delta region	90	30	17	14	5.2	4.6	3.4	103
2010-NJ[b]			91	44	18	14	4.3	4.1	3.3	111
Haze Region VI (SCB)										
Chengdu (CD) -2013	urban	Si Chuan Basin	166	79	24	25	14	11	6.6	94
2012-CD			141	64	23	21	12	9.0	5.7	100
Haze Region I (N. E. China)										
Dalian (DL) -2013	urban	Southern tip of Liaodong peninsula	101	58	13	11	8.5	4.0	3.2	69
2012-DL			89	52	14	10	8.8	4.2	2.8	89
Haze Region IX (N. W. China)										
Gaolanshan (GLS) -2013	rural	Gansu province	247	184	16	17	8.9	4.0	3.2	103
2012-GLS			157	102	15	15	7.3	3.9	2.4	99
Dunhuang (DH) -2013	rural	North margin of Kumutage Desert	240	201	9.1	24	2.5	0.65	2.5	68
2012-DH			198	162	6.6	20	2.5	0.81	2.3	70

[a] Classification of major haze regions referred from Zhang et al. (2012a);

[b] At XiAn and Nanjing here used are data in 2011 and 2010, respectively, for comaring with 2013 results;

[c] Beijing are 2009 data for PM_{10} and $PM_{2.5}$; Lasha data omitted because of no data of 2012 and 2013 for this station.

Title Page
Abstract | Introduction
Conclusions | References
Tables | Figures
|◀ | ▶|
◀ | ▶
Back | Close
Full Screen / Esc
Printer-friendly Version
Interactive Discussion

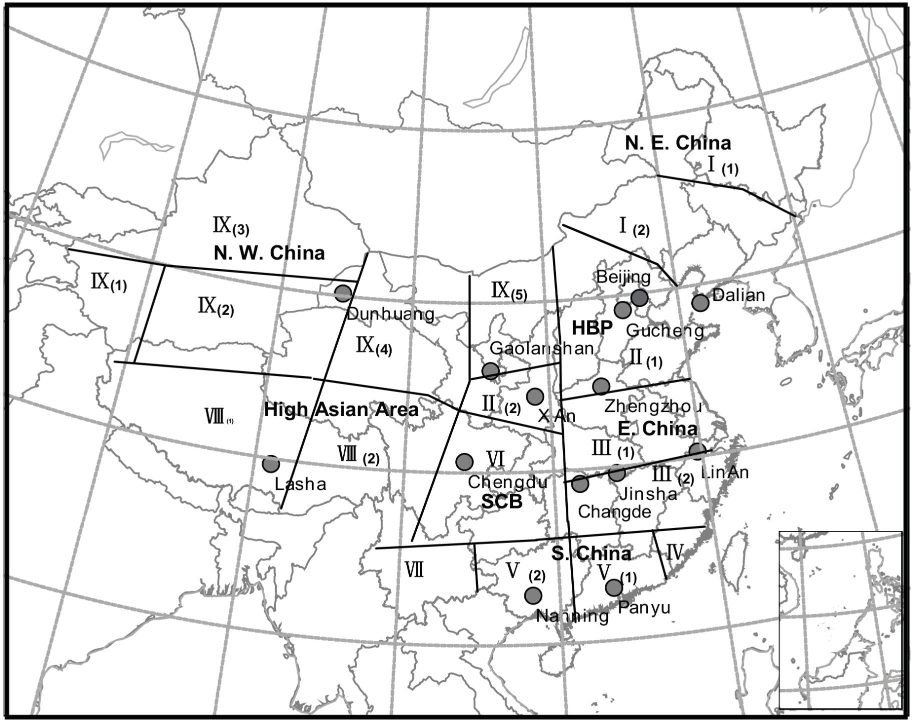

Figure 1. Locations of thirteen CAWNET stations and nine similar visibility changing regions in China (Zhang et al., 2012a).

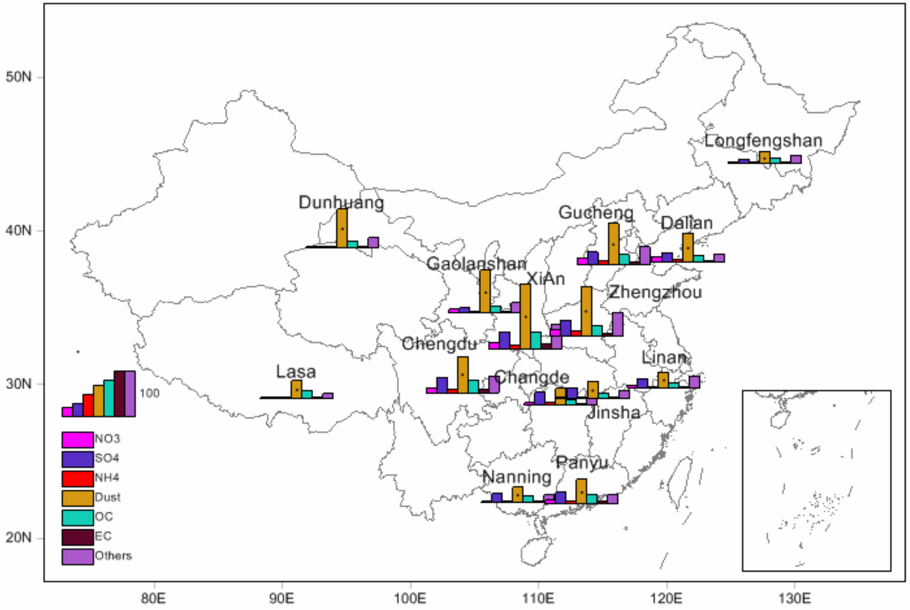

Figure 2a. Averaged mass concentrations of major chemical components in thirteen stations during 2006–2010.

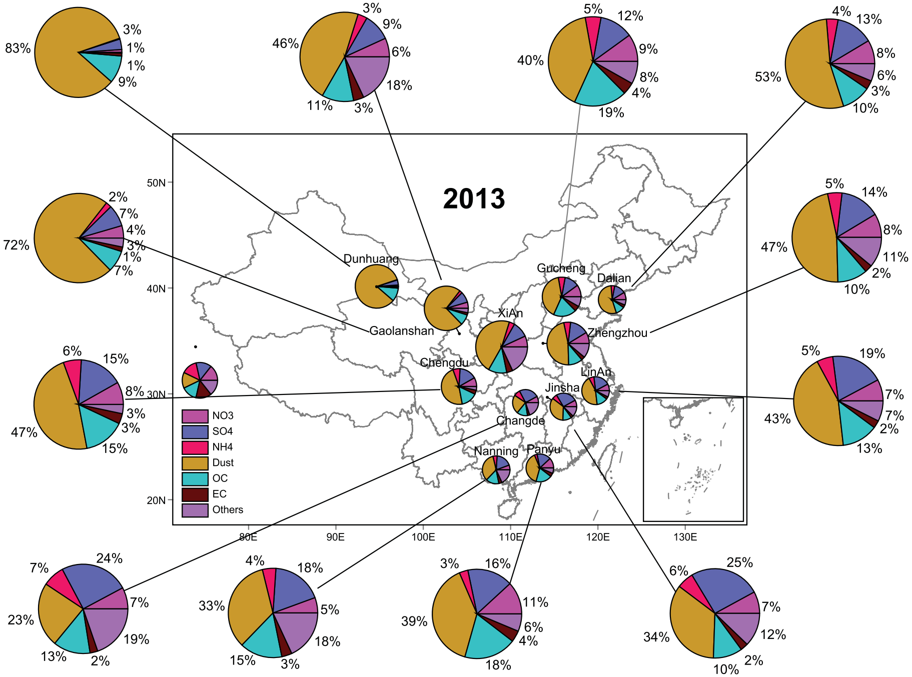

Figure 2b. Chemical proportions of PM_{10} in 2013.

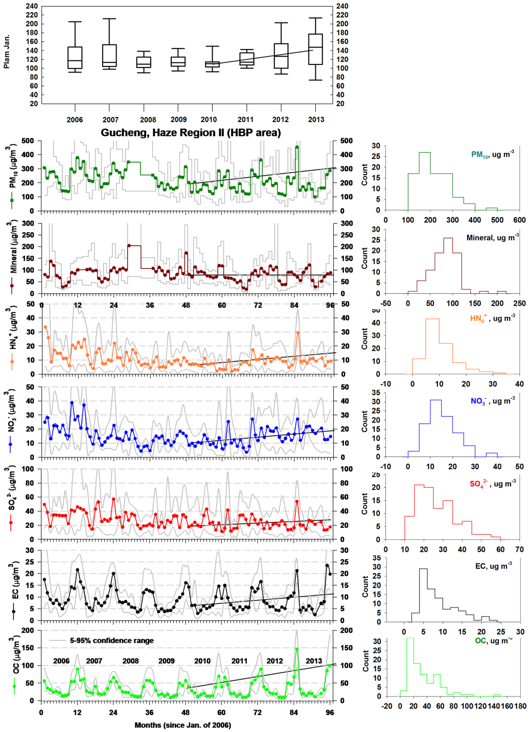

Figure 3. Left panel: change of monthly median concentrations of major chemical components, PM_{10}, and January PLAM at Gucheng in Haze Region II, one of major haze region in the Hua Bei Plain (HPB) area in China. Wintertime data were used in linear trend fitting from 2010 to 2013; right panel: histogram analysis for various chemical components.

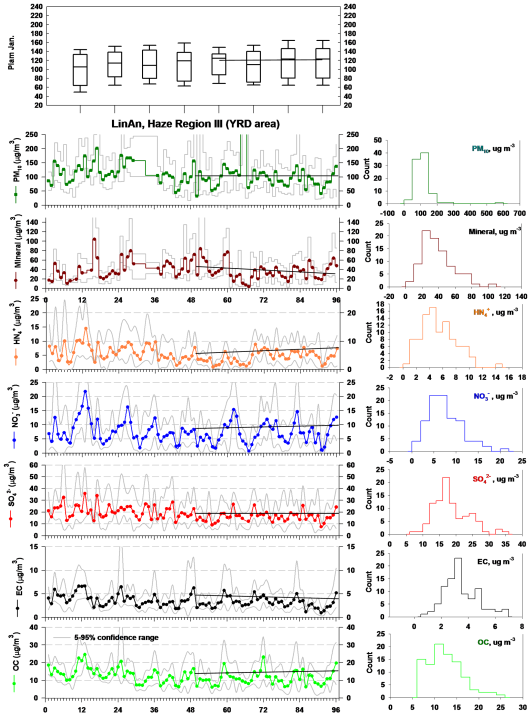

Figure 4. Left panel: change of monthly median concentrations of major chemical components, PM$_{10}$, and January PLAM at LinAn in Haze Region III, one of major haze region in the Yangtze River Delta (YRD) area in China. Wintertime data were used in linear trend fitting from 2010 to 2013; right panel: histogram analysis result for various chemical components.

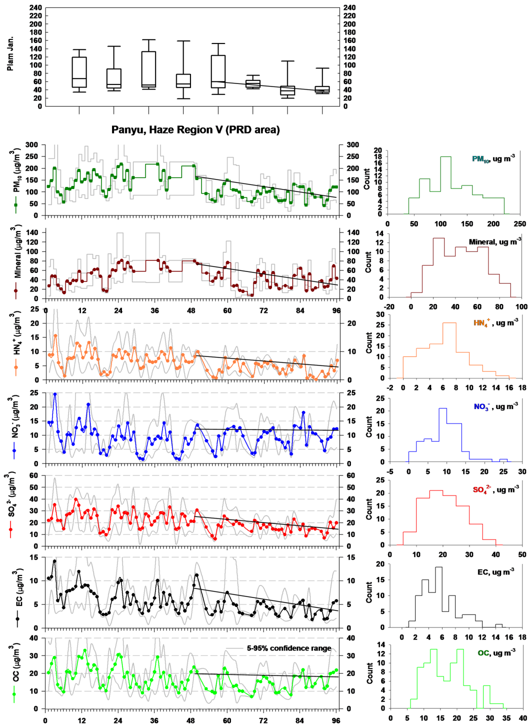

Figure 5. Left panel: change of monthly median concentrations of major chemical components, PM_{10}, and January PLAM at Panyu in Haze Region V, one of major haze region in the Pearl River Delta (PRD) area in China. Wintertime data were used in linear trend fitting from 2010 to 2013; right panel: histogram analysis result for various chemical components.

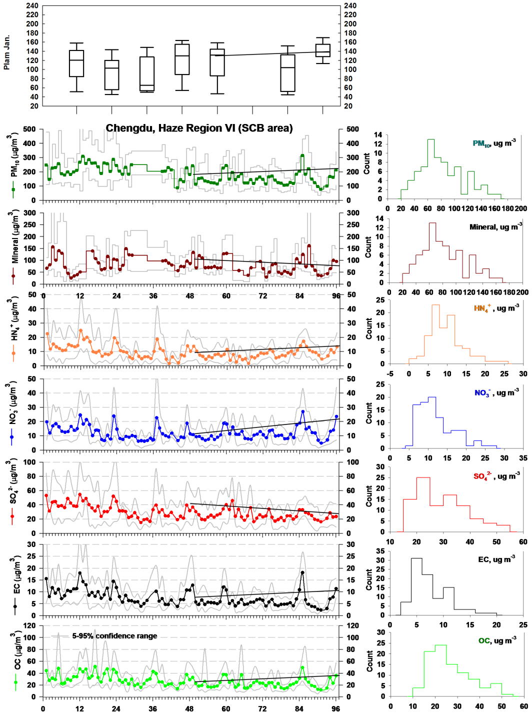

Figure 6. Left panel: change of monthly median concentrations of major chemical components, PM_{10}, and January PLAM at Chengdu in Haze Region VI, one of major haze region in the Si Chuan Basin (SCB) area in China. Wintertime data were used in linear trend fitting from 2010 to 2013; right panel: histogram analysis result for various chemical components.

ACPD
15, 19197–19238, 2015

Changes in chemical components of aerosol particles in different haze regions in China

X. Y. Zhang et al.

Title Page
Abstract Introduction
Conclusions References
Tables Figures
◀| |▶
◀ ▶
Back Close
Full Screen / Esc
Printer-friendly Version
Interactive Discussion